Functional Models for Catechol 1,2-Dioxygenase. Synthesis, Structure, Spectra, and Catalytic Activity of Certain Tripodal Iron(III) Complexes

Rathinam Viswanathan, Mallayan Palaniandavar,* Thailampillai Balasubramanian, and Thomas P. Muthiah

Department of Chemistry, Bharathidasan University, Tiruchirappalli 620024, Tamilnadu, India

Received June 6, 1997

A series of iron(III) complexes of tetradentate tripodal ligands [L1−H_2(L7); L1 = tris(pyrid-2-ylmethyl)amine, L2 = bis(pyrid-2-ylmethyl)(pyrid-2-ylethyl)amine, H(L3) = 2-bis(pyrid-2-ylmethyl)aminomethyl-4-nitrophenol, H_2(L4) = *N*,*N*-bis(2-hydroxy-5-nitrobenzyl)aminomethylpyridine, L5 = tris(benzimidazol-2-ylmethyl)amine, H(L6) = 2-bis(benzimidazol-2-yl)methylaminomethyl-4-nitrophenol, and H_2(L7) = *N*,*N*-bis(2-hydroxy-5-nitrobenzyl)-aminomethylbenzimidazole] have been synthesized. These complexes have been characterized using UV−vis spectral and electrochemical techniques. The single-crystal X-ray structure of [Fe(**L3**)Cl_2] has been determined by standard procedures and refined by least squares to a conventional *R* factor of 0.054. The violet crystals belong to the triclinic space group $P\bar{1}$ with $Z = 2$ and unit cell dimensions $a = 7.018(4)$ Å, $b = 9.087$ Å, and $c = 13.962(5)$ Å. The iron(III) complex has a pseudo-octahedral N_3OCl_2 donor set with two chloride ions occupying cis positions; the Fe−O(phenolate) bond is trans to one of the Fe−N_{py} bonds. The interaction of all the Fe(III) complexes with a variety of monodentate and bidentate heterocyclic bases as well as phenols has been investigated using electronic spectra. The interactions with catecholate anions reveal changes in the phenolate-to-iron(III) charge transfer band, similar to catechol dioxygenase−substrate complexes. The redox behavior of the complexes and their 1:1 adducts with 3,5-di-*tert*-butylcatechol (H_2DBC) has been investigated. All the complexes catalyze the oxidative cleavage of H_2DBC by molecular oxygen to yield *cis*,*cis*-muconic anhydride. The catalytic activity could be illustrated on the basis of the Lewis acidity of the complex−DBC adducts, derived from the CAT^{2-}/DBC^{2-} → Fe(III) CT band energy and the $E_{1/2}$ of the DBSQ/DBC couple, and steric hindrance to substrate binding and by assuming that the product release is the rate-determining phase of the reaction.

Introduction

The catechol dioxygenases are non-heme iron enzymes which catalyze the oxidative cleavage of catechols and serve as part of Nature's strategy for degrading aromatic molecules[1] in the environment. In the past decade several studies have been made to elucidate the structure−function relationship of these relatively unexplored metalloenzymes.[2,3] The intradiol-cleaving catechol dioxygenases, which catalyze the oxidative cleavage of catechols to *cis*,*cis*-muconic acids with the incorporation of molecular oxygen,[4] are represented by catechol 1,2-dioxygenase (CTD) and protocatechuate 3,4-dioxygenase (PCD) and are more extensively characterized than the extradiol-cleaving counterparts. Much interest has been shown in synthesizing iron(III) complexes to mimic the non-heme iron(III) coordination[5,6] environment, substrate interaction, and chemistry of the catalytic cycle of these enzymes. In early studies[7,8] Que and co-workers synthesized iron(III) complexes of *N*,*N*′-ethylenebis(salicylaldimine), which successfully mimicked many of the spectroscopic properties but not the catalytic activity of the enzymes. They also studied a series of [Fe(L)DBC] complexes,[9−11] where L is a tetradentate tripodal ligand like tris(pyrid-2-ylmethyl)-amine (TPA)[12] or nitrilotriacetic acid (NTA) or a NTA analogue with one or two carboxylate pendants and H_2DBC = 3,5-di-*tert*-butylcatechol. They found[10] that the Lewis acidity of the ferric center, as modulated by the tripodal ligand, plays an important role in dictating the rate of intradiol cleavage and the nature of products and their yields. On the basis of their prominent work they proposed a novel substrate rather than an oxygen activation mechanism[3,13,14] (Scheme 1) for the dioxygenase reaction, wherein the substrate loses both of its protons upon coordination to the iron(III) center followed by partial

* Author to whom correspondence should be addressed.

(1) *Microbial Degradation of Organic Molecules*; Gibson, D. T., Ed.; Marcel Dekker: New York, 1984; p 535.
(2) Feig, A. L.; Lippard, S. J. *Chem. Rev.* **1994**, *94*, 759.
(3) Que, L., Jr.; Ho, R. Y. N. *Chem. Rev.* **1996**, *96*, 2607.
(4) Lipscomb, J. D.; Orville, A. M. In *Metal Ions in Biological Systems*; Sigel, H., Sigel, A., Eds.; Marcel Dekker: New York, 1993; p 243.
(5) (a) Ohlendorf, D. H.; Lipscomb, J. D.; Weber, P. C. *Nature* **1988**, *336*, 403. (b) Ohlendorf, D. H.; Orville, A. M.; Lipscomb, J. D. *J. Mol. Biol.* **1994**, *244*, 586.
(6) (a) Que, L., Jr.; Lipscomb, J. D.; Zimmermann, R.; Munck, E.; Orme Johnson, W. H.; Orme-Johnson, N. R. *Biochim. Biophys. Acta* **1976**, *452*, 320. (b) Whittaker, J. W.; Lipscomb, J. D.; Kent, T. A.; Munck, E. *J. Biol. Chem.* **1984**, *259*, 4466. (c) Kent, T. A.; Munck, E.; Pyrz, J. W.; Widom, J.; Que, L., Jr. *Inorg. Chem.* **1987**, *26*, 1402.
(7) Que, L., Jr.; Heistand, R. H., II. *J. Am. Chem. Soc.* **1979**, *101*, 2219.
(8) Heistand, R. H., II; Lauffer, R. B.; Fikrig, E.; Que, L., Jr. *J. Am. Chem. Soc.* **1982**, *104*, 2789.
(9) Cox, D. D.; Que, L., Jr. *J. Am. Chem. Soc.* **1988**, *110*, 8085.
(10) Que, L., Jr.; Kolanczyk, R. C.; White, L. S. *J. Am. Chem. Soc.* **1987**, *109*, 5373.
(11) Cox, D. D.; Benkovic, S. J.; Bloom, L. M.; Bradley, F. C.; Nelson, M. J.; Que, L., Jr.; Wallick, D. E. *J. Am. Chem. Soc.* **1988**, *104*, 2026.
(12) It has been shown very recently that the non-heme Fe(II) complex of TPA catalyzes also the stereospecific alkane hydroxylation with H_2O_2. Kim, C.; Chen, K.; Kim, J.; Que, L., Jr. *J. Am. Chem. Soc.* **1997**, *119*, 5964.
(13) Que, L., Jr.; Lipscomb, J. D.; Munck, E.; Wood, J. M. *Biochim. Biophys. Acta* **1977**, *485*, 60.
(14) Que, L., Jr.; Lauffer, R. B.; Lynch, J. B.; Murch, B. P.; Pyrz, J. W. *J. Am. Chem. Soc.* **1987**, *109*, 5381.

S0020-1669(97)00708-8 CCC: $15.00
Published on Web 06/15/1998

Scheme 1. Diagram Showing the Substrate Activation Mechanism

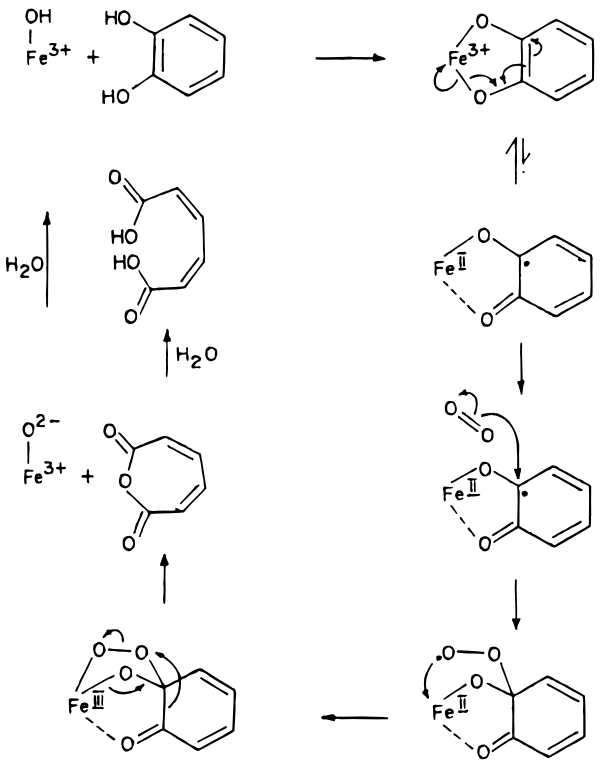

oxidation of the bound catecholate due to electron transfer from metal to ligand rendering the substrate with semiquinone character. The electrophilic[15] attack of dioxygen on the activated substrate yields a transient peroxy radical which combines with the equally short-lived iron(II) center to generate an alkylperoxoiron(III) species.[3,16] The peroxy adduct decomposes by a Criegee-type rearrangement to muconic anhydride.

Only two of the several tripodal ligand complexes recently reported[9,10,17,18] to effect oxidative cleavage contain a coordinated phenolate [H(L3), Chart 1]. No tripodal analogue reported so far contains one/two phenolic hydroxyl groups as well as imidazole nitrogen donor(s) though dioxygenases contain two tyrosine[5,19−21] and two imidazole[5,22] functions and a water molecule[23] or a hydroxide ion[24] coordinated to high-spin iron(III) in an environment intermediate between five- and six-coordination;[25] thus the X-ray crystal structure of PCD enzyme[5] reveals a trigonal bipyramidal geometry around iron(III). Further, even the highly reactive and catalyticaly active iron(III) catecholato complexes with tripodal[18] and macrocyclic[26] tetradentate ligands do not have a coordination environment which match that of the enzyme. Thus clearly no model reported so far possesses all the features of the dioxygenase active sites. So the present investigation aims at synthesizing and studying mononuclear Fe(III) complexes of systematically varied tetradentate tripodal ligands containing one or two phenolate functions along with benzimidazole (bzim) or pyridine (py) moieties (Chart 1). The present tripodal ligand systems are expected to generate the non-heme iron environment[5] of the enzymes. Our effort is directed toward investigating the phenolate-to-Fe(III) CT spectra and redox behavior of the complexes and their reactivity with H_2DBC. The present study is expected to afford improved understanding of enzyme−substrate complexes, verify the validity of the proposed oxidative cleavage mechanism for the present phenolate complexes, and thereby provide an assessment of the importance of tyrosinate coordination in the enzyme.

We have also determined the X-ray crystal structure of the analogue [Fe(L3)Cl_2] to illustrate the availability of two cis coordination sites for substrate binding and its catalytic activity.[17] This structure is the first one to contain one phenolate and two heterocyclic nitrogen donors coordinated to monomeric iron(III).

Experimental Section

Materials. Ferric chloride (anhydrous) and triethylamine (SD'S, Mumbai, India) were analytical grade reagents and were used as supplied. *o*-Phenylenediamine (Sisco, Mumbai, India), 2,2′-bipyridine (Merck, Mumbai, India), *N*-methylimidazole and 2-chloromethylpyridine hydrochloride (Fluka), 1,10-phenanthroline, catechol (Loba, Mumbai, India), 3,5-di-*tert*-butylcatechol and 2-chloromethylbenzimidazole (Aldrich), 2,9-dimethyl-1,10-phenanthroline (GFS), and dipicolylamine (Yamoto Yakuhin) were used as received. The supporting electrolyte *tetra-N*-hexylammonium perchlorate (GFS) was recrystallized twice from aqueous ethanol and used.

Synthesis of Ligands. 2-Aminomethylbenzimidazole dihydrochloride,[27] 2-hydroxy-5-nitrobenzyl chloride,[28] tris(pyrid-2-ylmethyl)amine[29] (L1), bis(benzimidazol-2-ylmethyl)amine,[30] and tris(benzimidazol-2-ylmethyl)amine[31] (L5) were synthesized by published procedures. 2-(2-Chloroethyl)pyridine hydrochloride was obtained by treating 2-(2-hydroxyethyl)pyridine with a slight excess of thionyl chloride, stirring overnight, and then destroying the excess thionyl chloride by heating with excess methanol. The required hydrochloride obtained was filtered, washed with methanol, and then dried over $CaCl_2$.

(15) In contrast to the intradiol-cleaving enzymes, the extradiol-cleaving enzymes, which require Fe^{II} for activity, have been very recently proposed to utilize an oxygen activation mechanism in which nucleophilic superoxide attacks the bound substrate. Ito, M.; Que, L., Jr. *Angew. Chem., Int. Ed. Engl.* **1997**, *36*, 1342.

(16) Support for the alkylperoxo−iron(III) species has been obtained. Bianchini, C.; Frediani, P.; Laschi, F.: Meli, A.; Vizza, F.; Zanello, P. *Inorg. Chem.* **1990**, *29*, 3402. Barbaro, P.; Bianchini, C.; Linn, K.; Mealli, C.; Meli, A.; Vizza, F.; Laschi, F.; Zanello, P. *Inorg. Chim. Acta* **1992**, *198*−*200*, 31. Barbaro, P.; Bianchini, C.; Mealli, C.; Meli, A. *J. Am. Chem. Soc.* **1991**, *113*, 3181. Such alkylperoxo species have been invoked in the mechanism of alkane functionalization catalyzed by non-heme iron complexes in concert with alkyl hydroperoxides. Kim, J.; Larka, E.; Wilkinson, E. C.; Que, L., Jr. *Angew. Chem., Int. Ed. Engl.* **1995**, *34*, 2048.

(17) Nishida, Y.; Shimo, H.; Kida, S. *J. Chem. Soc., Chem. Commun.* **1984**, 1611.

(18) Duda, M.; Pascaly, M.; Krebs, B. *J. Chem. Soc., Chem. Commun.* **1997**, 835.

(19) Que, L., Jr.; Heistand, R. H., II; Mayer, R.; Roe, A. L. *Biochemistry* **1980**, *19*, 2588.

(20) Que, L., Jr.; Epstein, R. M. *Biochemistry* **1981**, *20*, 2545.

(21) Siu, C.-T.; Orville, A. M.; Lipscomb, J. D.; Ohlendorf, D. H.; Que, L., Jr. *Biochemistry* **1992**, *31*, 10443.

(22) Felton, R. H.; Barrow, W. L.; May, S. W.; Sowell, A. L.; Goel, S. Bunker, G.; Stern, E. A. *J. Am. Chem. Soc.* **1982**, *104*, 6132.

(23) Whittaker, J. W.; Lipscomb, J. D., *J. Biol. Chem.* **1984**, *259*, 4487.

(24) True, A. E.; Orville, A. M.; Pearce, L. L.; Lipscomb, J. D.; Que, L., Jr. *Biochemistry* **1990**, *29*, 10847.

(25) (a) Walsh, T. A.; Ballou, D. P.; Mayer, R.; Que, L., Jr. *J. Biol. Chem.* **1983**, *258*, 14422. (b) Roe, A. L.; Schneider, D. J.; Mayer, R. J.; Pyrz, J. W.; Widom, J.; Que, L., Jr. *J. Am. Chem. Soc.* **1984**, *106*, 1676.

(26) (a) Koch, W. O.; Kruger, H.-J. *Angew. Chem., Int. Ed. Engl.* **1995**, *34*, 2928. (b) Koch, W. O.; Kruger, H.-J. *Angew. Chem., Int. Ed. Engl.* **1995**, *34*, 2671.

(27) Aminabhavi, T. M.; Biradar, N. S.; Patil, S. B. *Inorg. Chim. Acta* **1986**, *125*, 125.

(28) Horning, E. C., Ed. *Organic Syntheses*; Wiley: New York, 1955; Collect. Vol. III, p 468.

(29) Karlin, K. D.; Hayes, J. C.; Juen, S.; Hutchinson, J.; P. Zubieta, J. *Inorg. Chem.* **1982**, *21*, 4106.

(30) Usha, S.; Pandiyan, T.; Palaniandavar, M. *Indian J. Chem.* **1992**, *55*, 878.

(31) Thompson, L. K.; Ramaswamy, B. S.; Seymour, E. A. *Can. J. Chem.* **1977**, *55*, 878.

Chart 1. Ligand Structures L1−H_2(L7)

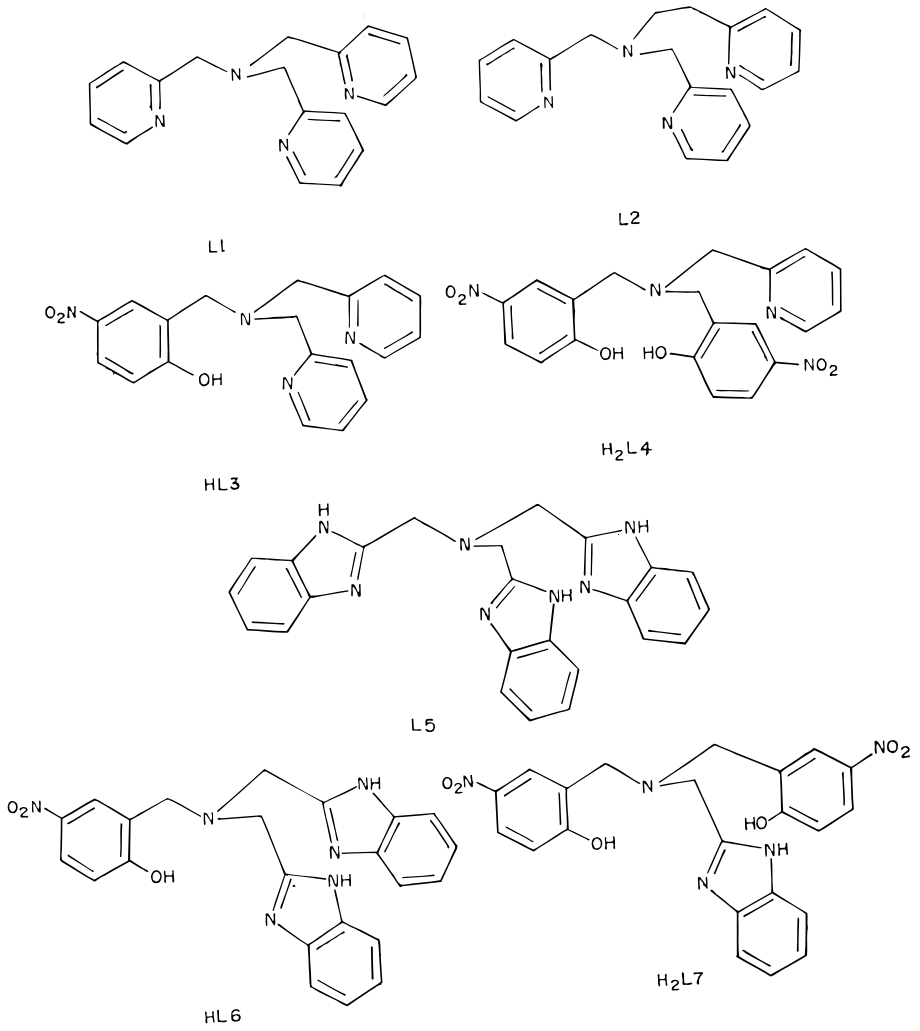

Preparation of Iron(III) Complexes. Fe(L1)Cl_3 [L1 = Tris(pyrid-2-ylmethyl)amine]. To a solution of bis(pyrid-2-ylmethyl)amine (0.80 g, 4 mmol) in THF (50 mL) was added 2-chloromethylpyridine hydrochloride (0.66 g, 4 mmol) followed by Et_3N (0.40 g, 4 mmol). The solution was refluxed for 30 min, cooled, and then filtered. The filtrate was evaporated to dryness, and then methanol (25 mL) was added, followed by $FeCl_3$ (0.65 g, 4 mmol) in methanol (2 mL). The precipitate obtained was filtered off, washed with cold methanol, and dried under vacuum. Yield: 1.3 g (78%). Anal. Calcd for $C_{18}H_{18}N_4Cl_3Fe$: C, 51.93; H, 4.35; N, 13.43. Found: C, 51.83; H, 4.14; N, 13.28.

Fe(L2)Cl_3 [L2 = Bis(pyrid-2-ylmethyl)(pyrid-2-ylethyl)amine]. This was prepared using the procedure for Fe(L1)Cl_3, starting from bis(pyrid-2-ylmethyl)amine and 2-(2-chloroethyl)pyridine hydrochloride. Yield: 1.25 g (72%). Anal. Calcd for $C_{19}H_{20}N_4Cl_2Fe$: C, 52.93; H, 4.68; N, 12.99. Found: C, 52.84; H,4.56; N, 12.87.

Fe(L3)Cl_2 [H(L3) = 2-Bis(pyrid-2-ylmethyl)aminomethyl-4-nitrophenol]. This complex was synthesized as described previously.[17] A methanolic solution of the complex was kept aside for slow evaporation at room temperature to obtain violet-colored single crystals suitable for X-ray diffraction.

Fe(L4)Cl·H_2O [H_2(L4) = *N*,*N*-Bis(2-hydroxy-5-nitrobenzyl)aminomethylpyridine]. To a solution of 2-hydroxy-5-nitrobenzyl chloride (0.75 g, 4 mmol) in THF (20 mL) was added 2-aminomethylpyridine (0.24 g, 2 mmol) with stirring, followed by Et_3N (0.40 g, 8 mmol). This was refluxed for 30 min, cooled, and then filtered. To the filtrate was added $FeCl_3$ (0.34 g, 2 mmol) in methanol (5 mL), and the mixture was stirred and then cooled. The solid that separated out was filtered off, washed with small amounts of MeOH, and dried under vacuum. Yield: 0.34 g (65%). Anal. Calcd for $C_{20}H_{18}N_4O_7ClFe$: C, 46.40; H, 3.50; N, 10.82. Found: C, 46.58; H, 3.68; N, 11.02.

Fe(L5)Cl_3 [L5 = Tris(benzimidazol-2-ylmethyl)amine]. To a solution of L5 (1.1 g, 4 mmol) in methanol (5 mL) was added $FeCl_3$ (0.65 g, 4 mmol) in methanol (2 mL). The solid obtained was filtered, washed with cold methanol, and dried under vacuum. Yield: 1.70 g (82%). Anal. Calcd for $C_{24}H_{23}N_7OCl_3Fe$: C, 55.78; H, 4.49; N, 18.97. Found: C, 55.63; H, 4.37; N, 18.82.

Fe(L6)Cl_2 [H(L6) = 2-Bis(benzimidazol-2-ylmethyl)aminomethyl-4-nitrophenol]. This was prepared using the procedure employed for Fe(L3)Cl_2 starting from 2-hydroxy-5-nitrobenzyl chloride and bis-(benzimidazol-2-ylmethyl)amine. Yield: 1.5 g (68%). Anal. Calcd for $C_{23}H_{19}N_6O_3Cl_2Fe$: C,49.85; H, 3.46; N, 15.16. Found: C,49.99; H, 3.52; N, 15.43.

Fe(L7)Cl·H_2O [H_2(L7) = *N*,*N*-Bis(2-hydroxy-5-nitrobenzyl)aminomethylbenzimidazole]. This was prepared using the procedure adopted for Fe(L4)Cl starting from 2-hydroxy-5-nitrobenzyl chloride and 2-aminomethylbenzimidazole. Yield: 0.40 g (71%). Anal. Calcd for $C_{22}H_{19}N_5O_7ClFe$: C, 47.46; H, 3.44; N, 12.58. Found: C, 47.35; H, 3.49; N, 12.70.

Instrumentation. Elemental analyses were performed at Hindustan Photo Film Manufacturing Co. Ltd, Ootacamund, India, and Regional Sophisticated Instrumentation Centre, Lucknow, India. Electronic spectra were recorded on a Hitachi U-3410 double-beam UV−vis−near-IR spectrophotometer. All voltammetric experiments were performed in a single-compartment cell with a three-electrode system on an EG & G PAR 273 potentiostat/galvanostat equipped with an IBM PS/2 computer and a HIPLOT DMP-40 series digital plotter. The working electrode was a glassy carbon disk (area 0.283 cm^2), and the

Table 1. Crystallographic Data for $[Fe(L3)Cl_2]$

empirical formula	$C_{19}N_4H_{17}FeCl_2O_3$
fw	476.12
space group	$P\bar{1}$ (triclinic, No. 2)
a	7.018(4) Å
b	9.087(3) Å
c	13.962(5) Å
α	80.22(6)°
β	84.33(3)°
γ	84.04(2)°
V	981.37 Å^3
Z	2
λ(Mo Kα)	0.710 69 Å
ρ_{calc}	1.611 g·cm^{-3}
no. of reflns measd	total: 3424 unique: 2564 (R_{int} = 0.0168)
R^a	0.054
$R_w{}^b$	0.099

^{a} $R = \sum||F_o| - |F_c||/\sum|F_o|$. ^{b} $R = \{\sum w[(F_o{}^2 - F_c{}^2)^2]/(\sum w[(F_o{}^2)^2]\}^{1/2}$.

reference electrode, saturated calomel. A Pt plate was used as the counter electrode. The supporting electrolyte used was 0.1 M THAP.

Solutions were deoxygenated by purging with N_2 gas for 15 min prior to measurements, and during measurements a stream of N_2 was passed over the solution. The temperature of the methanol solution was maintained at 25 ± 0.2 °C by a Haake D8 G circulating bath. The potential of the Fc/Fc^+ couple (0.087 V vs Ag/Ag^+) was measured in methanol under identical conditions to enable future correction for junction potentials.

Crystallographic Data Collection and Structure Analysis. Preliminary cell dimensions and the crystal system were determined and refined on an Enraf-Nonius CAD4 X-ray diffractometer. The intensities were collected on the same diffractometer with graphite-monochromated Mo Kα radiation. The crystal data and details of data collection are summarized in Table 1. The intensities of the representative reflections were measured after every 100 reflections. No decay correction was required. The data were corrected for Lorentz and polarization effects. An empirical absorption correction based on an ω scan was applied. The structure was solved by the SHELX-86 program[32] and the refinement by SHELXL-93.[33] E statistics suggested a centrosymmetric space group and the structure was solved in the space group $P\bar{1}$, which was confirmed by the successful refinement. The non-hydrogen atoms were refined anisotropically, and the hydrogen atoms were refined by using isotropic thermal parameters. Structural parameters such as bond lengths, bond angles, etc. were calculated using the program PARST.[34] All the calculations were carried out using MICROVAX-II. Selected bond lengths and bond angles are provided in Table 2, and the atomic coordinates for the non-hydrogen atoms are provided in Table 3. The atomic coordinates for the non-hydrogen atoms of the complex and Cl^- and their thermal parameters can be found in Tables S1, S3, and S4 (Supporting Information).

Reactivity Studies. The following typical procedure[17] was employed to study the dioxygenase activity of model compounds. A mixture of 3,5-di-*tert*-butylcatechol (1 mmol) and the iron(III) complex (0.02 mmol) in nitromethane solution (10 mL) was left in contact with air at room temperature for 4 days. The product was isolated by column chromatography on silica gel using chloroform as the eluent and was identified as *cis*,*cis*-muconic anhydride[35] (mp 93−95 °C, ν(C=O) 1745, 1765 cm^{-1}, λ_{max} 247 nm). The average of two determinations is reported.

Results and Discussion

Iron(III) complexes of a few tetradentate tripodal ligands based on trimethylamine [L1−H2(L7), Chart 1] with the pendant functionalities varying from py to bzim to phenolate have been synthesized to provide a systematic variation of the ligand Lewis basicity and charge while retaining similar coordination geometries in ternary complexes with catechols. Though the basicities of bzim and py groups are different from that of imidazole groups in proteins, the bulky bzim ring(s) seem to be a good choice to offer steric hindrance to the added ligands or substrates as in proteins. On the basis of the results of elemental analysis, the crystal structures of $[Fe(L3)Cl_2]$ (see below) and $[Fe(L5)Cl_2]Cl$,[36] and inferences from spectral studies, the structures of the present Fe(III) complexes may be assigned as octahedral,

Table 2. Selected Bond Distances (Å) and Angles (deg) for $[Fe(L3)Cl_2]$

Fe1−N2	2.195(3)	Fe1−N9	2.249(3)
Fe1−N16	2.196(3)	Fe1−O24	1.928(3)
Fe1−Cl1	2.330(2)	Fe1−Cl2	2.270(2)
C8−N9	1.480(5)	N9−C10	1.462(5)
C11−N16	1.350(5)	N9−C17	1.493(5)
C15−N16	1.343(6)	C23−O24	1.310(5)
O24−Fe1−Cl2	101.7(1)	N16−Fe1−Cl2	95.6(1)
N16−Fe1−O24	162.1(2)	N9−Fe1−O24	89.3(1)
N9−Fe1−N16	72.7(1)	N2−Fe1−Cl2	91.4(1)
N2−Fe1−Cl1	168.8(1)	N2−Fe1−O24	85.5(1)
N2−Fe1−N16	90.0(1)	N2−Fe1−N9	76.1(1)
Fe1−N2−C7	117.5(3)	Fe1−N2−C3	123.5(3)
N2−C7−C8	116.5(4)	C7−C8−N9	113.1(4)
Fe1−N9−C8	111.1(3)	C8−N9−C17	111.0(3)
C8−N9−C10	109.0(4)	Fe1−N9−C17	108.4(3)
Fe1−N9−C10	106.8(3)	C10−N9−C17	110.2(3)
N9−C10−C11	109.5(4)	Fe1−N16−C15	126.0(3)
N9−C17−C18	111.8(4)	Fe1−O24−C23	128.5(3)

Table 3. Atomic Coordinates ($\times 10^4$) and Equivalent Isotropic Displacement Parameters ($A^2 \times 10^3$) for $[Fe(L3)Cl_2]$

atom	x	y	z	U(eq)
Fe1	866(1)	1520(1)	2028(1)	29(1)
N2	3264(4)	845(3)	2715(2)	29(1)
C3	3568(6)	−470(5)	3314(3)	39(1)
C4	4950(6)	−781(6)	3838(3)	45(1)
C5	6090(6)	305(6)	3773(4)	45(1)
C6	5772(5)	1664(5)	3195(3)	36(1)
C7	4353(5)	1891(4)	2669(3)	30(1)
C8	4020(5)	3311(5)	1969(3)	34(1)
N9	2207(4)	3634(3)	1765(2)	29(1)
C10	2111(6)	4269(5)	734(3)	35(1)
C11	2560(5)	3044(4)	121(3)	33(1)
C12	3180(7)	3326(6)	−837(3)	47(1)
C13	3526(7)	2152(6)	−1358(3)	52(1)
C14	3238(7)	736(6)	−896(4)	50(1)
C15	2616(6)	523(5)	63(3)	40(1)
N16	2261(4)	1652(4)	581(2)	33(1)
C17	1298(6)	4691(4)	2393(3)	34(1)
C18	1396(5)	4090(4)	3459(3)	31(1)
C19	2144(5)	4817(4)	4061(3)	33(1)
C20	2144(5)	4264(4)	5044(3)	33(1)
C21	1347(6)	2988(5)	5457(3)	37(1)
C22	606(5)	2241(5)	4851(3)	36(1)
C23	622(5)	2723(4)	3860(3)	30(1)
O24	−46(3)	1980(3)	3287(2)	35(1)
N25	2978(5)	5057(4)	5666(3)	47(1)
O26	3594(5)	6230(4)	5291(2)	58(1)
O27	3038(5)	4536(4)	6524(2)	64(1)
Cl1	−1463(1)	2686(1)	1210(1)	42(1)
Cl2	301(2)	−908(1)	2150(1)	46(1)

(32) SHELX-86: Sheldrick, G. M. *Acta Crystallogr*. **1990**, *A46*, 467.
(33) SHELXL-93: Sheldrick, G. M. *SHELXL-93*; University of Gottingen: Gottingen, Germany, 1993.
(34) PARST, A System of Computer Routines for Calculation of Molecular Parameters from Results of Crystal Structure Analysis: Nordelli, M. Comput. Chem. **1983**, *7*, 95.
(35) Demmin, T. R.; Rogic, M. M. *J. Org. Chem*. **1980**, *45*, 4072.

(36) $[Fe(L5)Cl_2]Cl$ crystallized in the triclinic space group with a = 8.404(7) Å, b = 9.897(11) Å, and c = 15.006(10) Å; α = 86.73(9)°, β = 86.95(7)°, and γ = 80.39(9)°. The structure has been determined, and a tertiary amine, three benzimidazole nitrogens, and two chloride ions are coordinated to iron(III) in a distorted octahedral structure. The refinement of the crystal structure is in progress, and the complete details will be published elsewhere.

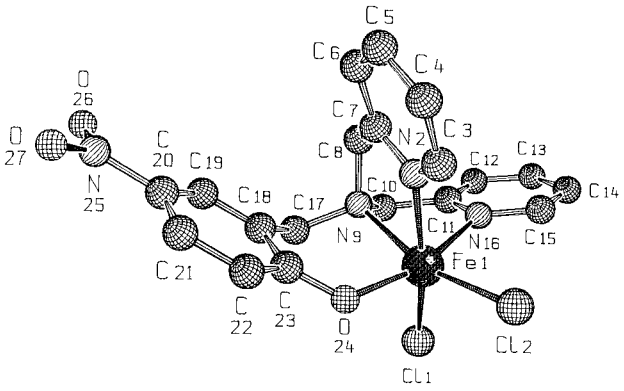

Figure 1. Perspective view of the complex $[Fe(L3)Cl_2]$ with atom-labeling scheme. The hydrogen atoms are omitted for clarity.

with the chloride ions coordinated. The conductivities of the complexes (Λ_M, 80−90 ohm^{-1} cm^2 mol^{-1} for [Fe(L)Cl], 145−210 ohm^{-1} cm^2 mol^{-1} for $[Fe(L)Cl_2]$, and 310−320 ohm^{-1} cm^2 mol^{-1} for $[Fe(L)Cl_3]$) reveal that the chloride ions are quite certainly not coordinated in methanol solution. This suggests that the complexes contain two readily replaceable cis coordination sites and hence are convenient for studying the effect of adduct formation on spectra. All the iron(III) complexes have magnetic moments in the range 5.5−5.8 μ_B at room temperature, consistent with a high-spin ferric center with five unpaired electrons.

Description of the X-ray Crystal Structure of $Fe(L3)Cl_2$. A perspective view[37] of the complex cation is shown in Figure 1, together with the atomic numbering scheme. The structure reveals an FeN_3OCl_2 coordination sphere with a distorted octahedral geometry. The tripodal ligand occupies four sites of the geometry, and two chloride ions occupy the remaining cis coordination positions. The phenolic oxygen atom occupies a coordination site trans to a py nitrogen and cis to the other. The tertiary amine nitrogen atom is trans to one of the chloride ions and is the farthest from iron [$Fe-N_{amine}$, 2.250(3) Å]. Both the py nitrogens are located at the same distance [$Fe-N_{py}$, 2.195(3), 2.197(3) Å] from iron. The shortest Fe−Cl distance is to the chloride (Cl2) axial to the FeN_2OCl1 plane: Fe−Cl2, 2.271(2) Å; Fe−Cl1, 2.330(2) Å. The $Fe-N_{py}$ and $Fe-N_{amine}$ distances are typical of octahedral Fe(III)−N distances of ∼2.15 Å[9,38−42] and are in the same range as those in the dimer $[Fe_2L_2O(OBz)]BPh_4$,[43] where H(L) [*N*-(*o*-hydroxybenzyl)-*N*,*N*-bis(pyrid-2-yl-methyl)amine] is analogous to H(L3), $[Fe(TPA)DBC]^+$,[44] $[Fe(NTA)DBC]^{2-}$,[10] and [Fe(BPG)DBC][9] [BPG = bis(pyrid-2-ylmethyl)glycine]. Further, the two pyridine nitrogens are cis to each other as in the dimeric structure of $[Fe_2L_2O(OBz)]BPh_4$;[43] in contrast, they are trans to each other in [Cu(L3)Cl][45] with a square pyramidal structure. The observed Fe−O(phenolate) distance of 1.928(3) Å is shorter than the octahedral Fe(III)-O distances of 1.98 Å,[9,38−42,46,47] suggesting stronger iron−oxygen overlap. It is also shorter than the Fe−N distances as expected, and the average of Fe−O/N bond lengths of 2.14 Å is typical of octahedral ferric model complexes[38−44,46,47] with oxygen and nitrogen ligation. Though the present tripodal ligand fails to impose a trigonal geometry around iron(III), its stereochemical requirement dictates that the Cl1−Fe1−N16 (83.2°) and O24−Fe1−N2 (84.5°) bond angles at the Fe vertex are significantly less than 90° and that the O24−Fe1−N16 (161.8°) and N9−Fe1−Cl2 (162.12°) bond angles are considerably less than 180°. While the former angular compression is directly linked with the large asymmetry in the Fe−Cl distances as well as the Cl1−Fe−Cl2 angle (99.30°), which is significantly higher than 90°, the latter is associated with the displacement of Fe by 0.14 Å away from the FeN_2OCl2 coordination plane. The phenolate oxygen in the six-membered chelate ring has an Fe1−O24−C23 bond angle of 128.5°, indicating that phenolate oxygen is sp^2 hybridized and aligned so that the out-of-plane $p\pi$ orbital can strongly interact with a half-filled $d\pi^*$ orbital on the Fe(III) ion.[41] The enhanced Fe−O overlap, as also discussed above, illustrates the higher molar absorptivity of the CT band (3000 M^{-1}, see below). The crystal structures of $[Fe(L3)Cl_2]$ and $[Fe(L5)Cl_2]Cl$ reveal that the two cis coordination sites in all the present complexes are available for coordination of two monodentate or one bidentate base molecule like DBC^{2-}. This is relevant to the hyperfine broadening observed from O^{17}-enriched water for the 4-HBA−PCD complex[48] (4-HBA = 4-hydroxybenzoate), which reveals that at least two coordination sites of Fe(III) appear adjacent and accessible to exogenous ligands. Further, studies[9,10,17−19] on biomimetic model complexes also reveal that two easily accessible cis coordination sites are needed for coordination of the catecholate ligand and its subsequent reaction with molecular oxygen.

Electronic Spectra. The electronic spectra of all the iron(III) phenolate complexes (Table 4) exhibit an intense band in the visible region (490−550 nm). This band is assigned[49] to the phenolate(π_1) → Fe(III)($d\pi$) CT transition as such a band is absent in complexes of L1, L2, and L5, which lack the phenolate function. The increasing order of energy of this visible band, Fe(L3) < Fe(L4); Fe(L6) < Fe(L7), represents the decreasing order of Lewis acidity of the ferric center because iron d-orbital energies are raised[11] by the negative charge built on Fe(III) due to the replacement of py/bzim by the second phenolate group. All these observations show that the band position as well as the intensity of the LMCT band is very sensitive to the iron environment. Significant changes in the visible band (Table 4) are observed on adding excess ligand molecules to ensure complete adduct formation. Addition of *N*-methylimidazole (mim) and bzim shifts the visible band to higher energies with a decrease in absorptivity for almost all the complexes. The addition of py also decreases the λ_{max} but enhances the absorptivity of compounds of bzim-based ligands. There is a blue shift with moderate to tremendous enhancement in absorptivity for the addition of bidentate heterocyclic bases, as expected; for 2,9-dimethyl-1,10-phenanthroline (DMP) there

(37) Schakal: A Fortran program for plotting crystal structures, Germany, 1992.
(38) Ainscough, E. W.; Brodie, A. M.; Plowman, J. E.; Brown, K. L.; Addison, A. W.; Gainsford, A. R. *Inorg. Chem.* **1980**, *19*, 3655.
(39) Lauffer, R. B.; Heistand, R. H., II; Que, L., Jr. *Inorg. Chem.* **1983**, *22*, 50.
(40) Malfant, I.; Morgenstern-Badrau, I.; Philoche-Lavisalles, M.; Lloret, F. *J. Chem. Soc., Chem. Commun.* **1990**, 1338.
(41) McDevitt, M. R.; Addison, A. W.; Sinn, E.; Thompson, L. K. *Inorg. Chem.* **1990**, *29*, 3425.
(42) Okamoto, K.-I.; Kanamori, K.; Hidaka, J. *Acta Crystallogr.* **1990**, *C46*, 1640.
(43) Yan, S.; Que, L., Jr.; Taylor, L. F.; Anderson, O. P. *J. Am. Chem. Soc.* **1988**, *110*, 5222.
(44) Jang, H. G.; Cox, D. D.; Que, L., Jr. *J. Am. Chem. Soc.* **1991**, *113*, 9200.
(45) Uma, R.; Viswanathan, R.; Palaniandavar, M.; Lakshmi Narayanan, M.; Manohar, H. *J. Chem. Soc., Dalton. Trans.* **1994**, 1219.
(46) Raymond, K. N.; Isied, S. S.; Brown, L. D.; Fronczek, F. R.; Nibert, J. H. *J. Am. Chem. Soc.* **1976**, *98*, 1767.
(47) Clarke, E. T.; Martell, A. E.; Reibenspies, J. *Inorg. Chim. Acta* **1992**, *196*, 177.
(48) (a) Whittaker, J. W.; Lipscomb, J. D. *J. Biol. Chem.* **1984**, *259*, 4487. (b) Orville, A. M.; Lipscomb, J. D. *J. Biol. Chem.* **1989**, *264*, 8791.
(49) Casella, L.; Gullotti, M.; Pintar, A.; Messouri, L.; Rockenbauer, A.; Gyor, M. *Inorg. Chem.* **1987**, *26*, 1031.

Table 4. $PhO^- \rightarrow$ Fe(III) CT Spectral Data[a] for the Adducts of Iron(III) Complexes in Methanol Solution

	λ_{max}, nm (ϵ, M^{-1} cm^{-1})				
added ligand	Fe(**L3**)Cl_2	Fe(**L4**)$Cl\cdot H_2O$	Fe(**L5**)Cl_3	Fe(**L6**)Cl_2	Fe(**L7**)$Cl\cdot H_2O$
none	550 (1650)	493 (630)	356 (4370)	500 (880)	492 (3120)
mim	467 (1350)	424 (610)	460 sh (530)	373 (910)	478 (7540)
bzim	479 (1510)	475 (580)	353 (3750)	382 (10 310)	478 sh (6240)
py	464 (1510)	480 (570)	350 (4330)	481 (1320)	478 (6730)
PhO^-	472 (2250)	389 (3320)	427 (6550)	470 sh (180)	396 (3090)
sal^- [e]	473 (4020)	480 (600)	463 sh (5130)	493 (980)	493 (1270)
bpy[f]	502 (4040)	480 (570)	520 (2200)	500 (2890)	467 (1270)
	472 sh (4370)		490 sh (2040)		
phen[g]	495 (4600)	485 (700)	506 (4310)	391 (11 810)	480 (7050)
			480 sh (3990)		
dmp	487 sh (2860)	480 (600)	485 (330)	494 (2360)	481 (6730)
			445 sh (1320)		
$CATH^-$	627 (5460)	670 (60)	520 (3620)	640 (980)	610 (6730)
		526 (680)		486 (2360)	500 (13 780)
$DBCH^-$	785 (3300)	700 (370)	670 sh (230)	760 (2130)	644 (4530)
				505 (1630)	483 (8810)

[a] Concentration of iron complexes: 3.3×10^{-4} M. [b] The ratio of added ligands to iron complexes was 10:1 for monodentate base and 5:1 for chelating base; the anions were generated by adding 1 equiv of methanolic NaOH to solutions containing the ligand and the iron complex in a 5:1 ratio. [c] Recorded under nitrogen, the monoanions and dianions were generated by adding the corresponding amounts of methanolic NaOH to dry methanol solution. [d] Consistent with ref 20. [e] Hsal = salicylaldehyde. [f] bpy = 2,2′-bipyridyl. [g] phen = 1,10-phenanthroline.

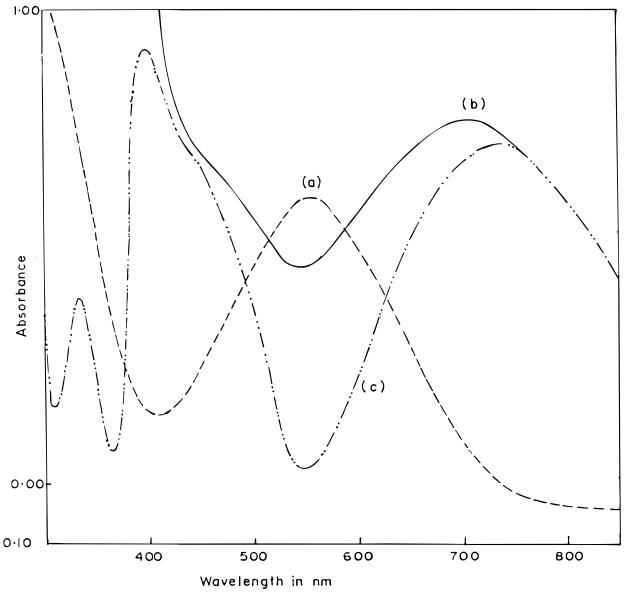

Figure 2. Absorption (vs methanol) spectra of [Fe(L3)Cl_2] (a) and [Fe(L3)DBC] (b) and difference spectrum (c) of [Fe(L3)DBC] vs [Fe(L3)Cl_2] in methanol.

is only a slight enhancement, possibly because of steric hindrance from its methyl groups for binding. The binding of phenolate (PhO^-) effects a large decrease in λ_{max} with increased or decreased absorptivity.

The appearance of two new bands (430−470, 630−890 nm) on the addition of CAT^{2-} or DBC^{2-} to all the iron(III) complexes is evident from the difference spectra (vs the original complex), rather than the absorbance spectra (vs methanol) of the catecholate adducts (Figure 2, Table 5). Since different ligand orbitals of catecholates are involved in LMCT transitions, two $CAT^{2-}/DBC^{2-} \rightarrow$ Fe(III) CT bands are expected, as observed[11] for $[Fe(L1)DBC]^-$ (578, 888 nm) and $[Fe(L5)DBC]^-$ (548, 842 nm). Obviously, the high energy $CAT^{2-}/DBC^{2-} \rightarrow$ Fe(III) CT band would have merged with the original phenolate $\rightarrow$ Fe(III) CT band, now blue-shifted on adduct formation. The blue shift in the latter band indicates the conversion of catecholate ligand to a fairly basic ligand, which would be consistent with peroxide species[50] in the proposed mechanism (Scheme 1). Further, the difference spectral features are similar to those observed[11] for the interaction of catechol with phenylalanine hydroxylase (PAH) (410, 700 nm) and for that of soybean lipoxygenase with 4-nitrophenol (395, 630 nm) and protocatechuic acid (455, 670 nm); this suggests that the Lewis acidity of the iron center in the present synthetic complexes with one phenolate hydroxyl, rather than in those with two such groups or those with three py or bzim pendants, is comparable to those in the enzyme−substrate complexes. This lends support to the speculation[11] that the above enzymes contain two neutral histidine groups[51] and one acidic donor like carboxylate oxygen in the six-coordinate iron(III) active site. However, it is cautioned that the replacement of carboxylate by phenolate has been shown[9] to change the coordination environment significantly and affect the Lewis acidity and hence reactivity. Very recently Solomon et al.[52] have invoked significant oxygen ligation and long Fe−N/O bond distances to illustrate the low ligand field strength and the XAS and EXAFS patterns of the $\{Fe^{3+}\}$PAH enzyme. Further, interestingly, the average of the Fe−O/N bond distances (2.14 Å) observed for the [Fe(L3)Cl_2] complex is close to these distances.

The energies of the above LMCT bands observed for DBC^{2-} adducts are lower than those for CAT^{2-} adducts; the electron-donating *tert*-butyl groups would raise[11] the energy of the catecholate frontier orbitals and thus minimize the ligand-to-metal energy gap. Further, on the addition of even neutral H_2-DBC rather than H_2CAT the CT bands are exhibited, of course, with relatively low absorptivity. On the addition of Et_3N to deprotonate H_2DBC the absorptivities are enhanced. This reveals the spontaneous deprotonation of H_2DBC rather than H_2CAT to bind strongly to the Lewis acidic Fe(III) center. Also the spectral data obtained for $HDBC^-$ addition indicates that the complex species generated in solution are only those containing coordinated DBC^{2-}. The low-energy CAT^{2-}, $DBC^{2-} \rightarrow$ Fe(III) CT band exhibits remarkable dependence on the

(50) Pyrz, J. W.; Roe, A. L.; Stern, L. J.; Que, L., Jr. *J. Am. Chem. Soc.* **1985**, *107*, 614.
(51) The presence of two histidine residues at the sites of PAH has been recently suggested on the basis of mutagenesis studies, with carboxylate oxygen and a solvent oxygen completing the coordination sphere. Gibbs, B. S.; Wojchowski, D.; Benkovic, S. J. *J. Biol. Chem.* **1993**, *268*, 8046.
(52) Loeb, K. E.; Westre, T. E.; Kappock, T. J.; Mitic, N.; Glasfeld, E.; Caradonna, J. P.; Hedmann, B.; Hodgson, K. O.; Solomon, E. I. *J. Am. Chem. Soc.* **1977**, *119*, 1901.

Table 5. LMCT Spectral Data for Catecholate and DBC^{2-} Adducts of Iron(III) Phenolate Complexes in Methanol Solution

	λ_{max}, nm (ϵ, M^{-1} cm^{-1})			
added ligand[a]	Fe(**L3**)Cl_2	Fe(**L4**)$Cl\cdot H_2O$	Fe(**L6**)Cl_2	Fe(**L7**)$Cl\cdot H_2O$
none	550 (1650)	495 (630)	500 (880)	492 (3120)
$CATH_2$ (vs complex[b])	540 (280)	900 (60)	784 (110)	850−650[c]
	550 (−140)	500 (−15)	400 (−240)	500 (−250)
CAT^{2-}	710 (2020)	642 (180)	660 (730)	510 (500)
	460 (2380)		505 (740)	
CAT^{2-} (vs complex[b])	730 (1920)	683 (220)	655 (530)	663 (80)
	560 (−80)	520 (−180)	470sh (1650)	500 (−320)
	450sh (1910)			
$DBCH_2$ (vs complex[b])	800 (60)	825−550[c]	800 (250)	474 (60)
	400 (150)		558 (200)	
DBC^{2-}	790 (490)	850−700[c]	768 (360)	800−600[c]
	490sh (670)		492 (510)	
DBC^{2-} (vs complex[b])	795 (600)	743 (460)	777 (570)	780−550[c]
	560 (−80)	520 (−50)	550 (−100)	520 (−300)
	450sh (410)	440sh (90)	485sh (400)	

[a] Concentration of iron(III) complexes: 4.16×10^{-4} M. The ratio of the added ligands to iron(III) complexes was 1:1. The catecholate anions were generated by adding 2 equiv of Et_3N to solutions containing the catechol and the iron complex in a 1:1 ratio. [b] Difference spectrum. [c] Very broad band.

Table 6. Electrochemical Data[a] for the Parent and DBC^{2-}-Bound[b] Complexes [Fe(L)DBC] in Methanol at 25 ± 0.2 °C Using a Scan Rate of 50 mV/s

				$E_{1/2}$ (V)		
compd	E_{pc} (V)	E_{pa} (V)	ΔE_p (mV)	CV	DPV[c]	redox process
$Fe(L1)Cl_3$	0.036	0.158	122	0.097	0.078	$Fe^{III} \rightarrow Fe^{II}$
$[Fe(L1)DBC]^+$ [d]		0.578			0.615	DBQ/DBSQ
	−0.778	−0.032			−0.773	$Fe^{III} \rightarrow Fe^{II}$
$Fe(L2)Cl_3$	0.018	0.112	94	0.065	0.060	$Fe^{III} \rightarrow Fe^{II}$
$[Fe(L2)DBC]^+$		0.584			0.348	DBQ/DBSQ
	−0.134	0.006	140	0.070	−0.052	DBQ/DBSC
	−0.780				−0.760	$Fe^{III} \rightarrow Fe^{II}$
$Fe(L3)Cl_2\cdot H_2O$	−0.144	−0.046	98	−0.095	−0.101	$Fe^{III} \rightarrow Fe^{II}$
$[Fe(L3)DBC]^{2-}$		0.694			0.597	DBQ/DBSQ
	0.064	0.044	108	−0.010	0.008	DBQ/DBSC
	−0.674				−0.597	$Fe^{III} \rightarrow Fe^{II}$
$Fe(L4)Cl\cdot H_2O$	−0.376	−0.244	132	−0.310	−0.301	$Fe^{III} \rightarrow Fe^{II}$
$[Fe(L4)DBC]^-$		0.582			0.580	DBQ/DBSQ
	−0.240	−0.140	100	−0.190	−0.210	DBQ/DBSC
	−0.612				−0.673	$Fe^{III} \rightarrow Fe^{II}$
$Fe(L5)Cl_3$	−0.032	−0.036	68		−0.002	$Fe^{III} \rightarrow Fe^{II}$
$[Fe(L5)DBC]^+$		0.440			0.393	DBQ/DBSQ
	−0.402	−0.032	370		−0.054	DBQ/DBSC
	−0.608				−0.551	$Fe^{III} \rightarrow Fe^{II}$
$Fe(L6)Cl_2$	−0.204	−0.074	130	−0.139	−0.130	$Fe^{III} \rightarrow Fe^{II}$
$[Fe(L6)DBC]^{2-}$		0.628			0.610	DBQ/DBSQ
		−0.046			−0.130	DBQ/DBSC
	−0.574				−0.483	$Fe^{III} \rightarrow Fe^{II}$
$Fe(L7)Cl\cdot H_2O$	−0.346	−0.256	90	−0.301	−0.301	$Fe^{III} \rightarrow Fe^{II}$
	0.204[e]					
$[Fe(L7)DBC]^-$		0.618			0.588	DBQ/DBSQ
		−0.198			−0.240	DBQ/DBSC
	−0.614				−0.513	$Fe^{III} \rightarrow Fe^{II}$

[a] E in volts vs $Ag/AgNO_3$ (0.01 M, 0.1 M THAP); add 0.544 V to convert to NHE. [b] Generated by adding to complex 1 and 2 equiv of DBC and Et_3N, respectively. [c] Pulse height: 25 mV. [d] Difficult to locate DBSQ/DBC couple. [e] Additional anodic peak.

nature of the tetradentate tripodal ligand, and the band shifts to higher energy as the softer nitrogen ligand is replaced by pendant phenolate: Fe(L1) ≈ Fe(L2) < Fe(L3) < Fe(L4); Fe(L5) < Fe(L6) < Fe(L7); this is consistent with the decrease in Lewis acidity of the iron center.

Electrochemical Behavior. All the parent chloride complexes show a cathodic (0.036 to −0.376 V, Table 6) as well as an anodic wave (−0.046 to −0.244 V), and the values of current functions ($D = 1.0-3.5 \times 10^{-6}$ g/cm^2) are of the same order as those observed[53] for a one-electron-reduction process. The i_{pc} vs $\nu^{1/2}$ plot is linear, but the values of peak current ratio i_{pa}/i_{pc} (1.0−0.6) and peak potential separation ΔE_p (68−132 mV) suggest fairly reversible to irreversible redox processes. The values of Fe(III)/Fe(II) redox potentials of the complexes follow the orders Fe(L1) > Fe(L2) >Fe(L3) > Fe(L4); Fe(L5) > Fe(L6) > Fe(L7); this reflects the decreasing Lewis acidity of the iron(III) center as the charge on the tetradentate tripodal ligand set increases. This trend is consistent with that derived from $CAT^{2-}/DBC^{2-} \rightarrow$ Fe(III) and $PhO^- \rightarrow$ Fe(III) LMCT band energies, and in fact, the present data fit into the straight line (Figure 5) obtained when $PhO^- \rightarrow$ Fe(III) LMCT band energies

(53) (a) Viswanathan, R.; Palaniandavar, M. *J. Chem. Soc., Dalton Trans.* **1995**, 1259. (b) Palaniandavar, M.; Viswanathan, R. *Proc. Indian Acad. Sci., Chem. Sci.* **1996**, *108*, 235.

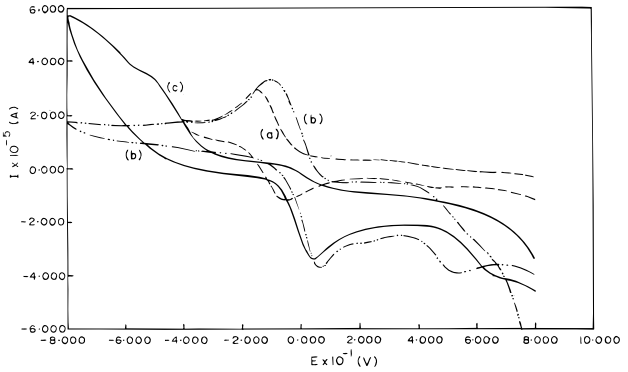

Figure 3. Cyclic voltammograms of 1 mM [Fe(L3)Cl_2] (a), with 1 mM DBC added (b) and 3 mM Et_3N added (c) in methanol at a scan rate of 0.05 V/s. Supporting electrolyte: 0.1 M THAP.

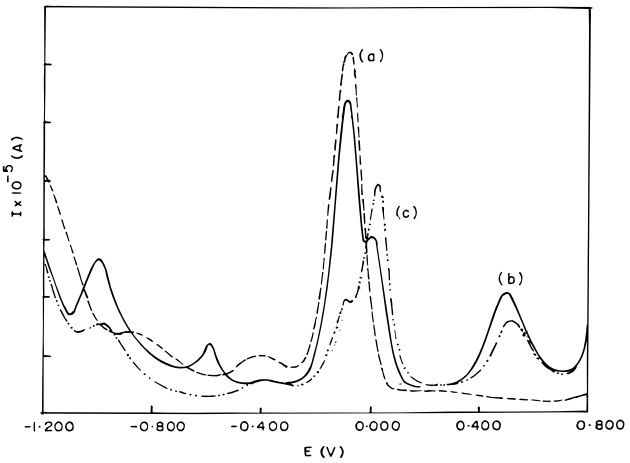

Figure 4. Differential pulse voltammograms of 1 mM [Fe(L3)Cl_2 (a), with 1 mM DBC added (b) and 1 mM Et_3N added (c) in methanol at a scan rate of 0.001 V/s. Supporting electrolyte: 0.1 M THAP.

are plotted against $E_{1/2}$ of Fe(III) complexes of certain linear tridentate phenolate ligands[53] containing pyridyl/benzimidazolyl functions.

The adducts $[Fe(L)DBC]^{n-}$ were generated in methanol solution for electrochemical investigation. The cyclic (Figure 3) and differential pulse (Figure 4) voltammetric results corresponding to their complete formation as evidenced by spectral measurements are collected in Table 6. For some of these adducts, only the oxidation wave of the DBSQ/DBC couple[54] is discernible. The redox potential of this couple (0.008 to −0.240 V) is significantly more positive than that (−0.890 V, NHE)[55] of free H_2DBC, reflecting considerable stabilization of H_2DBC by chelation to ferric center. Also it is more positive than, and exhibits the same trend as, that of the Fe(III)/Fe(II) couple of the parent complex and reflects the Lewis acidity of the iron center in $[Fe(L)DBC]^{n-}$, which decreases with the increase in number of coordinated phenolate groups and on replacing the more effectively π-back-bonding py by the bzim group. Similar variations in DBSQ/DBC redox potentials have been associated with differing Lewis acidities of ferric centers in $[Fe(L)DBC]^{n-}$ complexes as modulated by the tripodal ligand L.[9,56] For the present complexes these potentials are more positive than those for $[Fe(salen)DBC]^-$ (−0.179 V, NHE)[56] and $[Fe(NTA)DBC]^{2-}$ (−0.024 V, NHE)[57] adducts, which exhibit catechol cleavage activity. This suggests that all the present compounds should show cleavage activity.

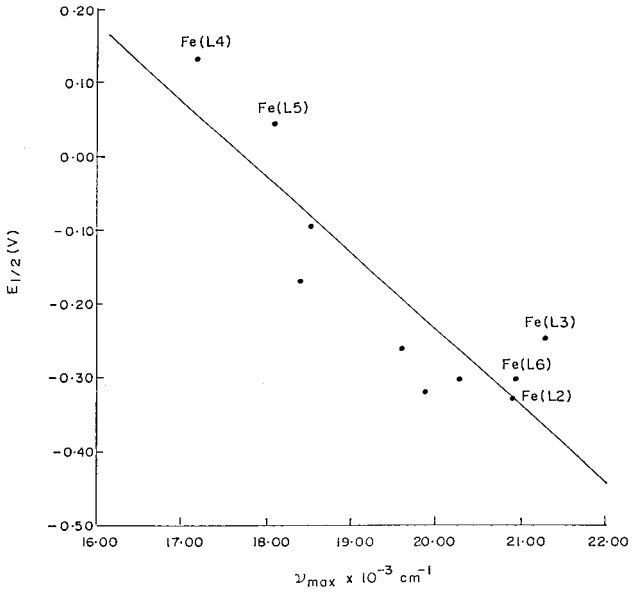

Figure 5. Linear correlation of $E_{1/2}(Fe^{III}/Fe^{II})$ with phenolate-to-iron(III) CT band energies for the present iron(III) complexes and for those of tridentate phenolates.[53]

The incorporation of a coordinated phenolate depresses the $E_{1/2}$ of the Fe^{III}/Fe^{II} couple of the parent complexes by 40−200 mV, and the coordination of DBC^{2-} depresses the $E_{1/2}$ by 100−500 mV; this reflects the decrease in Lewis acidity of the iron center on substrate binding and supports the suggestion that the Fe(III) center in the dioxygenases not only participates in the activation of the substrate but also facilitates the latter stages of the reaction. Further, the $E_{1/2}$ of the substrate-coordinated Fe(III) center reflects the reducibility of the center to form the oxide anion (Scheme 1).[13]

Catalytic Activity of Model Compounds. The oxidative intradiol cleavage of H_2DBC was observed when it was mixed with the present iron(III) compounds in nitromethane solution in the molar ratio 50:1 and kept for 4 days. The complexes act as catalysts in this reaction, because the amounts of product obtained [Fe(L1), 41%; Fe(L2), 45%; Fe(L3),[58] 12%; Fe(L4), 56%; Fe(L5), 18%; Fe(L6), 59%; Fe(L7), 50%] were more than that of the complex used. The yields show a dependence on the nature of the tetradentate ligand, revealing that the coordination chemistry of the iron(III) center plays a role in determining the course of the O_2 reaction. Thus the yields for Fe(L1) and Fe(L2) are higher than that for Fe(L5), possibly due to a decrease in Lewis acidity and an increase in steric hindrance to substrate binding on replacing py by the bzim pendant. Again, a decrease in Lewis acidity on going from Fe(L1)/Fe(L2) to Fe(L3) appears to decrease the yield. This is in line with the earlier observation[10] of Que et al. that the incorporation of a phenolate donor in the iron coordination environment diminishes the Lewis acidity of the iron center and hence the yield of the cleavage product. It has been rationalized[3] that a decrease in Lewis acidity of the iron center decreases the covalency of the iron−catecholate interaction and decreases the semiquinone character (Scheme 1) of bound DBC^{2-}. The present observation also supports the proposal[10] that the increased yield of the desired

(54) Johnson, C. R.; Henderson, W. W.; Shepherd, R. F. *Inorg. Chem.* **1984**, *23*, 2754.
(55) Nanni, E. J.; Stallings, M. D.; Sawyer, D. T. *J. Am. Chem. Soc.* **1980**, *102*, 4481.
(56) Lauffer, R. B.; Heistand, R. H., II; Que, L., Jr. *J. Am. Chem. Soc.* **1981**, *103*, 3947.
(57) White, L. S.; Nilsson, L. H.; Pignolet, L. H.; Que, L., Jr. *J. Am. Chem. Soc.* **1984**, *106*, 8312.
(58) The observed yield is in agreement with that observed earlier.[17]

cleavage product with increased Lewis acidity of the metal center reflects the coordination[16] of the intermediate peroxide (Scheme 1) to the metal center. On the other hand, a similar decrease in Lewis acidity on introducing one phenolate donor, as in Fe(L6), or two phenolate donors, as in Fe(L4) and Fe(L7), tends to increase the yield. This is consistent with the observation[4] that the rate-determining phase of the enzyme reaction is product release and not oxygen attack or ring opening. If the dissociation of the Fe−O(substrate) bond in the oxygenated product in the novel substrate activation mechanism[3,13,14] (Scheme 1) proposed by Que et al. is the rate-determining step, then it would be facilitated by the increased negative charge built on the iron centers in Fe(L4) and Fe(L7) complexes. This is supported by the very recent finding of Krebs et al.[18] that electron-donating substituents on catechol result in a higher dioxygenase reactivity. However, the isolation and study of the kinetics[9] of the cleavage of the DBC^{2-} adducts of the present complexes are essential to clarify the above observations. Thus, though the observed yields of desired cleavage product could not be illustrated solely on the basis of the Lewis acidity of complexes, all the present observations are consistent with the above substrate activation mechanism.

Conclusion and Relevance to Iron Oxygenases. One of the important conclusions of the present model studies is that not only the phenolate-to-iron(III) CT band but also the CAT^{2-}/DBC^{2-} → Fe(III) CT band is remarkably sensitive to the primary ligand environment. These conclusions are similar to those arrived at by Que et al.[3,6−8] When H_2CAT or H_2DBC is added to a solution of the present iron(III) complexes, the absorption band in the region (400−500 nm) of phenolate-to-iron(III) CT was broadened with a remarkable increase in absorbance in the range 600−750 nm. This behavior strikingly resembles that of substrate complexes[7,59] of PCD or CTD enzymes in steady state conditions; however, the latter show a negligible increase or even a slight decrease of absorption in the 400−500 nm region. The difference spectra of the CAT^{2-} and DBC^{2-} adducts of the present complexes containing labile chlorides clearly show that catechol binding to iron(III) occurs with definite changes in iron coordination environment but without any concomitant displacement of coordinated phenolate of the primary ligand. Similar conclusions have been made from our studies[53] on iron(III) complexes of certain linear tridentate phenolates. However, very recent resonance Raman and crystal structure studies[3] on a PCD enzyme substrate complex suggest that the axial tyrosinate and the coordinated hydroxide are replaced on substrate interaction. Further, the catechol binding studies have been useful in diagnosing the coordination environment of the iron site in non-heme iron enzymes such as PAH, which lack iron−phenolate coordination. The appearance of the DBC^{2-} → Fe(III) CT band and the DBSQ/DBC redox wave and the lowering of the Fe(III)/Fe(II) redox potential on adding H_2DBC, even in the absence of added base, demonstrate the spontaneous deprotonation of the latter on binding to iron. This is consistent with one of the suggested functions of the iron(III) center in the enzyme, viz., promoting the loss of both protons of the substrate. Also this is relevant to the observation that the presence of catechol lowers the potential of the iron(III) center in the enzyme and renders it difficult to reduce under biological conditions.[60] The present study leads to emphasize the role the phenolate ligands play in modulating the Lewis acidity of the iron(III) center and determining the course and yield of the catalytic intradiol cleavage reaction, and it reveals the validity of the substrate activation mechanism of intradiol cleavage for iron(III) phenolate complexes. The use of the present non-heme iron(III) complexes as catalysts for alkane functionalization[61] to model the reactivity of non-heme iron centers in enzymes such as methane monooxygenase is under current investigation.

Acknowledgment. We thank the Council of Scientific and Industrial Research, New Delhi, for supporting this research (Scheme No: 9(299)/90 EMR-II dt.14.02.90) and for a fellowship to one of us (R.V.) [9/475(25)91 EMR 1] and Dr. S. Ananthapadmanabhan, Hindustan Photo Films Ltd, Ooty, for C,H,N analysis. We thank Dr. B. Varghese and Dr. T. Manisekaran for X-ray data collection and Regional Sophisticated Instrumentation Centre, Indian Institute of Technology, Madras, for EPR and X-ray diffraction facilities. We thank one of the referees for pointing out certain important references.

Supporting Information Available: Tables of fractional atomic coordinates, thermal parameters, and bond lengths and angles (3 pages). Ordering information is given on any current masthead page.

IC970708N

(59) Felton, R. H.; Cheung, L. D.; Philips, R. S.; May, S. W. *Biochem. Biophys. Res. Commun.* **1978**, *85*, 844.

(60) Que, L. Jr.; Lipscomb, J. D.; Zimmermann, R.; Munck, E.; Orme-Johnson, N. R.; Orme-Johnson, W. H. *Biochim. Biophys. Acta* **1976**, *452*, 320.

(61) Kim, J.; Harrison, R. G.; Kim, C.; Que, L., Jr. *J. Am. Chem. Soc.* **1996**, *118*, 4373.